Anal. Chem. **1997,** *69,* 4156−4161

An Ion Trap Interface for ESI−Ion Mobility Experiments

Cherokee S. Hoaglund, Stephen J. Valentine, and David E. Clemmer*

Department of Chemistry, Indiana University, Bloomington, Indiana 47405

A method for improving the sensitivity of ion mobility measurements of ions generated from continuous ionization sources such as electrospray ionization is described. The method involves an ion trap interface between the continuous source and the pulsed experiment. The trap allows the electrosprayed ion beam to be accumulated between pulses of the mobility experiment and provides tightly focused (both spatially and temporally) ion pulses for initiating experiments. Using this method, we have improved signal-to-noise ratios by factors of ∼10−30 compared with those of existing approaches and achieved experimental duty cycles of nearly 100%. With these improvements, it is possible to record complex ion mobility distributions in less than 10 s, and we have obtained detection limits of 1.3 pmol for the oligosaccharide maltotetraose. A detailed description of the experimental arrangement is given. An application of the improved methods in which collision-induced fragmentation of biomolecules is monitored by ion mobility spectrometry is described.

Recently, electrospray ionization (ESI)[1] sources for mass spectrometry (MS) have been coupled with ion mobility techniques[2−9] in order to examine the conformations of large biomolecules in the gas phase.[10] An intrinsic limitation of the ESI−ion mobility combination is that ESI is a continuous ion source, while ion pulses are required for mobility measurements. It is typical to discard 99−99.9% of the ion signal during the mobility experiment, making these methods inherently insensitive. Recent improvements in the resolving power of these instruments require the use of shorter pulses or longer times between pulses;[11] this reduces the duty cycle. Thus, it has become important to address how to increase the efficiency of these measurements. In this paper, we describe an ion trap[12] interface for the ESI−ion mobility experiment that offers significant advantages in instrument performance. This interface is similar to one that has been recently developed for ESI−time-of-flight (TOF) MS experiments.[13−15] Here, we show that the ESI−ion trap interface is a simple means of concentrating ions during the drift tube measurements; this provides duty cycles that approach 100% and improvements in signal-to-noise (S/N) ratios (compared with existing methods) by factors of ∼10−30. The ion trap also provides ion pulses that are tightly focused both spatially and temporally, allowing ions to be efficiently injected into the ion mobility instrument.

A number of MS-based techniques are currently being used to study the structures of biological ions in the gas phase, including measurements of hydrogen/deuterium exchange levels,[16−19] proton-transfer reactivity,[20] ion scattering experiments in triple-quadrupole instruments,[21−24] microscopy studies of the hillocks formed on surfaces after being exposed to high-energy ion collisions,[25,26] measurements of kinetic energy release,[27−29] and measurements of ion mobilities.[10,30−37] The ESI−ion mobility method is a versatile approach. Direct structural information can

(1) Fenn, J. B.; Mann, M.; Meng, C. K.; Wong, S. F.; Whitehouse, C. M. *Science* **1989**, *246*, 64.
(2) Hagen, D. F. *Anal. Chem.* **1979**, *51*, 870.
(3) Tou, J. C.; Boggs, G. U. *Anal. Chem.* **1976**, *48*, 1351.
(4) Karpas, Z.; Cohen, M. J.; Stimac, R. M.; Wernlund, R. F. *Int. J. Mass Spectrom. Ion Processes* **1986**, *83*, 163.
(5) St. Louis, R. H.; Hill, H. H. *Crit. Rev. Anal. Chem.* **1990**, *21*, 321.
(6) Wittmer, D.; Chen, Y. H.; Luckenbill, B. K.; Hill, H. H. *Anal. Chem.* **1994**, *66*, 2348.
(7) von Helden, G.; Hsu, M. T.; Kemper, P. R.; Bowers, M. T. *J. Chem. Phys.* **1991**, *95*, 3835.
(8) Jarrold, M. F. *J. Phys. Chem.* **1995**, *99*, 11.
(9) Clemmer, D. E.; Jarrold, M. F. *J. Mass Spectrom.* **1997**, *32*, 577.
(10) Clemmer, D. E.; Hudgins, R. R.; Jarrold, M. F. *J. Am. Chem. Soc.* **1995**, *117*, 10141.
(11) Dugourd, P.; Hudgins, R. R.; Clemmer, D. E.; Jarrold M. F. *J. Sci. Instrum.* **1997**, *119*, 3558.
(12) Discussions of ion traps have been given previously. See, for example: Paul, W.; Steinwedel, H. *U.S. Patent* 2939952, 1960. March, R.; Huges, R. *Quadrupole Storage Mass Spectrometry*; Wiley: New York, 1989. Cooks, R. G.; Kaiser, R. E., Jr. *Acc. Chem. Res.* **1990**, *23*, 213. Glish, G. L.; McLuckey, S. A. *Int. J. Mass Spectrom. Ion Processes* **1991**, *106*, 1. March, R. E. *J. Mass Spectrom.* **1997**, *32*, 351.
(13) Michael, S. M.; Chien, M.; Lubman, D. M. *Rev. Sci. Instrum.* **1992**, *63* (10), 4277.
(14) Michael, S. M.; Chien, B. M.; Lubman, D. M. *Anal. Chem.* **1993**, *65*, 2614.
(15) Quian, M. G.; Lubman, D. M. *Anal. Chem.* **1995**, *67*, 234A.
(16) Winter, B. E.; Light-Wahl, K. J.; Rockwood, A. L.; Smith, R. D. *J. Am. Chem. Soc.* **1992**, *114*, 5897.
(17) Suckau, D.; Shi, Y.; Beu, S. C.; Senko, M. W.; Quinn, J. P.; Wampler, F. M.; McLafferty, F. W. *Proc. Natl. Acad. Sci. U.S.A.* **1993**, *90*, 790.
(18) Wood, T. D.; Chorush, R. A.; Wampler, F. M.; Little, D. P.; O'Connor, P. B.; McLafferty, F. W. *Proc. Natl. Acad. Sci. U.S.A.* **1995**, *92*, 2451.
(19) Cassady, C. J.; Carr, S. R. *J. Mass Spectrom.* **1996**, *93*, 3143.
(20) For a recent review, see: Williams, E. R. *J. Mass Spectrom.* **1996**, *31*, 831.
(21) Covey, T. R.; Douglas, D. J. *J. Am. Soc. Mass Spectrom.* **1993**, *4*, 616.
(22) Collings, B. A.; Douglas, D. J. *J. Am. Chem. Soc.* **1996**, *118*, 4488.
(23) Chen, Y.-L.; Collings, B. A.; Douglas, D. J. *J. Am. Soc. Mass. Spectrom.*, in press.
(24) Cox, K. A.; Julian, R. K.; Cooks, R. G.; Kaiser, R. E. *J. Am. Soc. Mass Spectrom.* **1994**, *5*, 127.
(25) Quist, A. P.; Ahlbom, J.; Reimann, C. T.; Sundquist, B. U. R. *Nucl. Instru. Methods in Phys. Res. B* **1994**, *88*, 164.
(26) Sullivan, P. A.; Axelsson, J.; Altmann, S.; Quist, A. P.; Sundquist, B. U. R.; Reinmann, C. T. *J. Am. Soc. Mass Spectrom.* **1996**, *7*, 329.
(27) Kaltashov, I. A.; Fenselau, C. C. *J. Am. Chem. Soc.* **1995**, *117*, 9906.
(28) Adams, J.; Strobel, F.; Reiter, A. *J. Am. Soc. Mass Spectrom* **1996**, *7*, 30.
(29) Kaltashov, I. A.; Fenselau, C. C. *Proteins* **1997**, *27*, 165.
(30) von Helden, G.; Wyttenbach, T.; Bowers, M. T. *Science* **1995**, *267*, 1483.
(31) Wyttenbach, T.; von Helden, G.; Bowers, M. T. *J. Am. Chem. Soc.* **1996**, *118*, 8355.
(32) . Shelimov, K. B.; Clemmer, D. E.; Hudgins, R. R.; Jarrold, M. F. *J. Am. Chem. Soc.* **1997**, *119*, 2240.
(33) Shelimov, K. B.; Jarrold, M. F. *J. Am. Chem. Soc.* **1997**, *119*, 2987.
(34) Valentine, S. J.; Clemmer, D. E. *J. Am. Chem. Soc.* **1997**, *119*, 3558.

S0003-2700(97)00526-X CCC: $14.00

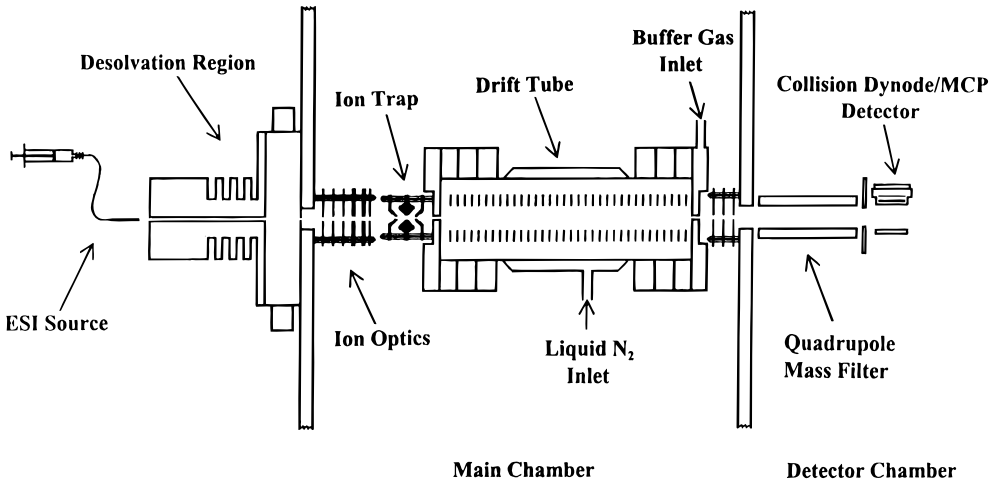

Figure 1. Schematic diagram of the experimental apparatus.

be obtained by comparing experimentally measured collision cross sections with those that are calculated for trial conformations.[10] It is possible to investigate the dynamics of conformational changes[32−36] as well as the chemical reactivity of shape-resolved conformations.[34−37] For example, when protein ions are injected into the drift tube at elevated kinetic energies, they undergo structural changes that correspond to folding and unfolding transitions,[32−36] which can be recorded in the ion mobility distribution. Mobilities are measured at high pressures (∼2−5 Torr), making it possible to vary the buffer gas temperature in order to measure Arrhenius activation energies for structural transitions.[9,38] Information about the chemical reactivities of differently shaped protein conformations have been carried out by doping the buffer gas with reagent gasses. By adding deuterated solvents to the buffer gas, it is possible to monitor the number of accessible heteroatom hydrogens at the surface of compact and elongated conformers of cytochrome *c*.[34] Equilibrium binding enthalpies for the first water molecules that associate with these conformers have also been measured.[37] Virtually any type of biomolecule can be examined, and these methods have recently been extended to study the gas-phase geometries of oligosaccharides[39] and DNA.[40]

As mentioned above, the present work is closely related to recent advances in ESI−TOFMS measurements.[13−15] Lubman and co-workers have shown that the ESI−ion trap combination facilitates duty cycles near 100% for TOFMS, significantly improving S/N ratios, sensitivity, and mass resolution.[14] The shortcomings of this approach arise from different pressure requirements for the ion trap (10^{-4}−10^{-3} Torr) and flight tube (<10^{-7} Torr) regions of the instrument. Here, we show that similar advantages can be gained by utilizing an ion trap for ESI−ion mobility experiments. Additionally, the pressure requirements for the trap are accommodated by mounting it on the drift tube entrance flange; in these studies, it fills from buffer gas that leaks out of the drift tube entrance. This makes installation of the trap a minor instrumental alteration; thus, it seems that the ion trap interface for ESI−ion mobility experiments is an even more suitable match than the "marriage made in MS".[15]

Another approach that has been explored as a means of improving the duty cycle of ion mobility measurements is to record the ion mobility distribution as an interferogram by utilizing two ion gates at different locations in the drift tube.[41] In principle, duty cycles as high as 50% can be achieved;[42] however, so far this approach has not been widely employed.

EXPERIMENTAL SECTION

General. A schematic diagram of our experimental apparatus is shown in Figure 1. The instrument is comprised of four basic components: (1) an ESI source, for formation of ions; (2) an ion trap, for ion accumulation and ejection; (3) a variable temperature drift tube, for separation of ions; and (4) a quadrupole MS/detection system. Each of these components is described in detail below. A brief overview of the experimental sequence is as follows. A low-energy ion beam formed by ESI is focused into the entrance of the ion trap. The ion trap continuously accumulates ions and periodically ejects the trapped ions into the entrance of a drift tube containing ∼2−5 Torr of a buffer gas. The pulse of ions drifts through the gas under the influence of a uniform electric field, and different species are separated on the basis of differences in their mobilities through the gas. Ions that exit the drift tube are focused into a quadrupole/MS detection system, and ion mobility distributions are recorded using a multichannel scaler.

Ion formation. For the description of the ion trap interface, we report studies of the four-residue sugar, maltotetraose (α-D-Glc*p*-(1→4)-α-D-Glc*p*-(1→4)-α-D-Glc*p*-(1→4)-D-Glc, Sigma, 95% purity). The experimental approach should be general for studying biomolecular ions. We briefly examined several other systems with the ion trap, including deprotonated α-cyclodextrin, cytochrome *c*, and apomyoglobin, although, at this point, no attempt has been made to optimize or characterize the advantages of utilizing the trap for these systems. Negatively charged (deprotonated) maltotetraose ions were formed at atmospheric pressure by electrospraying a solution containing ∼10^{-4} M oligosaccharide

(35) Valentine, S. J.; Anderson, J.; Ellington, A. E.; Clemmer, D. E. *J. Phys. Chem. B* **1997**, *101*, 3891.
(36) Valentine, S. J.; Counterman, A. E.; Clemmer, D. E. *J. Am. Soc. Mass Spectrom.*, in press.
(37) Woenckhaus, J.; Mao, Y.; Jarrold, M. F. *J. Phys. Chem. B* **1997**, *101*, 847.
(38) Jarrold, M. F., unpublished results.
(39) Liu, Y.; Clemmer, D. E. *Anal. Chem.* **1997**, *69*, 2504.
(40) Hoaglund, C. S.; Liu, Y.; Ellington, A. E.; Pagel, M.; Clemmer, D. E. *J. Am. Chem. Soc.*, in press.
(41) Knorr, F. J.; Eatherton, R. L.; Siems, W. F.; Hill, H. H., Jr. *Anal. Chem.* **1985**, *57*, 402.
(42) Shvartsburg, A. A.; Jarrold, M. F., unpublished results.

solution in 49:49:2 water/acetonitrile/ammonium hydroxide. Charged droplets enter a variable-temperature, differentially pumped desolvation region (~1−10 Torr) through a 0.025 cm diameter aperture. Ions exit this region through another 0.025 cm diameter aperture and enter the main vacuum chamber of the instrument. A series of diagnostic studies with and without buffer gas in the drift tube shows that this method primarily forms deprotonated parent ions. Under some conditions, a small fraction of singly charged dimers (up to ~25% of the total ion signal) are also observed.

Trapping Ions. Ions exiting the source are focused into a low-energy ion beam and guided into an ion trap (R. M. Jordan, Model C-1251). The ion trap consists of three electrodes: two endcaps and a center ring. The entrance and exit endcaps have 0.32 and 0.16 cm diameter apertures, respectively, that allow ions to enter and exit the trap. The electrodes are isolated by ceramic guard rings which seal the trapping region (except for the entrance and exit holes) and are mounted directly to the entrance plate of the drift tube on four 0.64 cm long alumina standoffs. In this configuration, the trap confines ions to a small volume in its center, which is in alignment with the entrance aperture of the drift tube. Ions are ejected from the trap into the drift tube without additional focusing.

Ions continuously enter the trap (except during the short ejection pulse) through a 0.32 cm diameter entrance, where they experience a 1.1 MHz rf field that is applied to the ring electrode. The magnitude of the field can be varied from 0 to 5000 V (peak-to-peak), depending on the m/z ratios of the ions that are being trapped. The buffer gas pressure inside the trap ($\sim 10^{-4}-10^{-3}$ Torr) is supplied from buffer gas (nitrogen or helium) that leaks out of the entrance of the drift tube and ambient gas pressure in the main chamber. In these studies, background pressures in the main chamber due primarily to residual buffer gas were varied from $\sim 5 \times 10^{-4}$ to 8×10^{-4} Torr (as measured with an ionization gauge in the main chamber) by changing the drift tube pressure, with no noticeable effect on the performance of the ion trap.

Voltages to the endcaps and ring electrodes are supplied by an ion trap power supply (R. M. Jordan, D-1203). In order to trap ions, the trap is biased within a few volts of the potential at the exit of the ESI source. Ions are ejected out of the trap by turning off the rf field and supplying a short (0.6 μs) dc pulse to one of the endcaps. In the present configuration, ions are ejected by supplying a negative pulse to the entrance electrode using a remote pulse amplifier that can be varied to ±400 V. Studies as a function of ejection pulse voltage over a 40−400 V range, and variations in the time between turning off the rf field and applying the pulse (from 0.2 to ~4 μs), had no significant effect on the ion signal. We also found that the ion signal was less sensitive to focusing conditions of the pretrap lens system than it was to focusing of these lenses without the trap. We presume this is a result of the large entrance aperture (0.32 cm diameter) of the trap and its ability to tightly focus ions for injection into the smaller drift tube aperture. A key parameter in these studies is the bias voltage of the trap. In all of our studies, ions were trapped and ejected within a narrow bias voltage window (less than 30 V). Outside of this range, ions either were not ejected or continuously leaked out of the trap.

Drift Tube. The drift tube is 32.4 cm long with 0.16 diameter entrance and exit apertures. The body is constructed of stainless steel with Teflon spacers at each end for electrical isolation of the entrance and exit plates. A uniform electric field is provided by 26 equally spaced electrostatic lenses, made of a 0.010 cm thick BeCu alloy, that are connected by 5 MΩ glass-sealed resistors (KDI Electronics) suitable for high vacuum. The drift tube body is constructed of concentric tubes that provide a cavity that can be filled by an external source of liquid nitrogen or a heating fluid. The ion mobility distributions shown below were recorded using ~2−5 Torr of 300 K nitrogen buffer gas and a drift field of 43.2 V cm^{-1}.

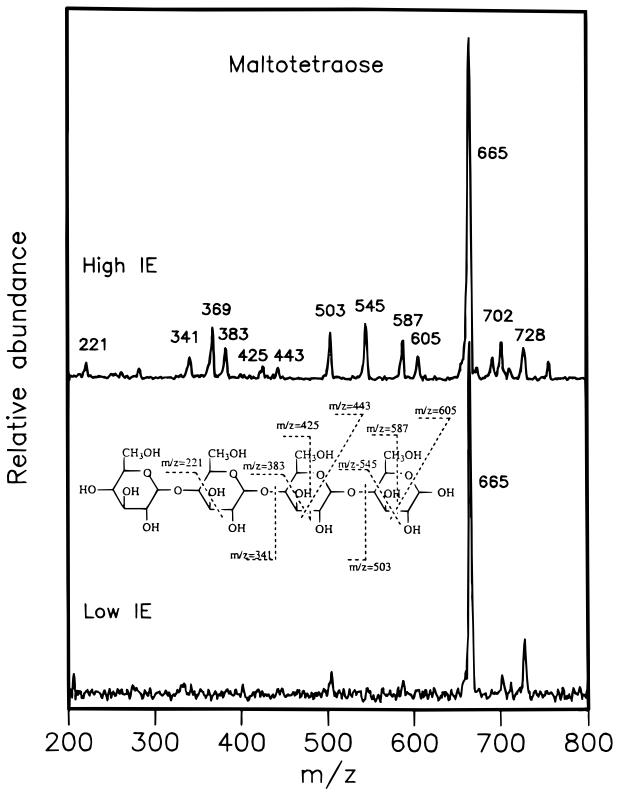

Figure 2. Mass spectra of negatively charged (deprotonated) maltotetraose recorded upon injecting ions into a drift tube containing nitrogen as the buffer gas at low injection energies (~400 eV) and high injection energies (~1200 eV). The schematic diagram delineates the bond cleavages necessary to form each of the observed fragment ions.

Quadrupole/Detector. After exiting the drift tube, ions are focused into a quadrupole mass spectrometer (Extrel) that can be set to transmit all ions or a specific m/z ion for recording ion mobility distributions. The quadrupole can be scanned in order to record mass spectra. The m/z limit of the quadrupole is 4000, with near unit resolution. Ions are detected using an off-axis collision dynode/dual-microchannel plate detection system that was designed and constructed in-house.

RESULTS AND DISCUSSION

Collision-Induced Dissociation of Maltotetraose. When maltotetraose ions are injected into the drift tube, they are rapidly heated as their kinetic energy is thermalized by collisions with the buffer gas. Further collisions cool the ions to the buffer gas temperature. This process can induce fragmentation at the entrance of the drift tube, making it possible to record ion mobility distributions for fragment ions. Figure 2 shows example mass spectra for deprotonated maltotetraose ions that have been injected into the drift tube at low and high injection energies. At low injection energies, the spectrum is dominated by the parent

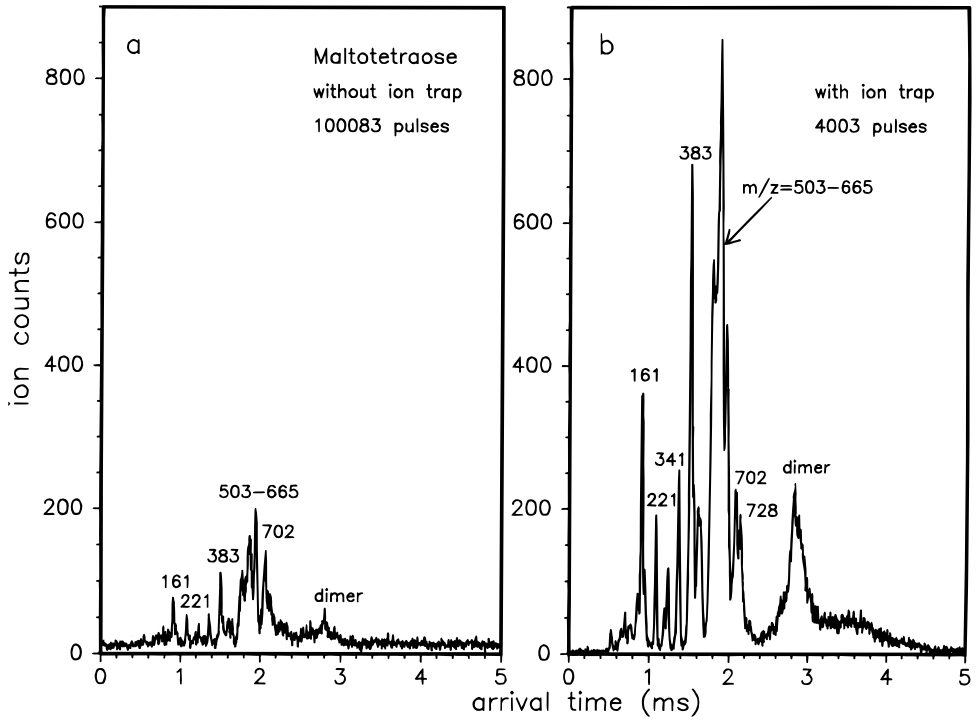

Figure 3. Ion mobility distributions recorded for maltotetraose and related fragments formed upon injection of ions at high injection energies into a drift tube containing ~2 Torr of nitrogen buffer gas. The dwell time resolution of the multichannel scaler was 5 μs/bin for these data. Part a shows the distribution that was acquired without the ion trap, using a pulse width of 20 μs for 100 083 pulses over an 11 min acquisition time. Part b shows the ion mobility distribution recorded with the ion trap using an rf trapping potential of 3000 V_{p-p}. The pulse width was ~1 μs, and a trapping time of 165 ms was used. The data shown correspond to 4003 pulses and also required an acquisition time of 11 min. Individual peaks are labeled with values of their mass-to-charge ratios determined in separate experiments by recording ion mobility distributions for mass selected ions. See text for details.

ion at $m/z = 665$. As the injection energy is increased, a series of fragment ions is observed. The scheme in Figure 2 delineates a pattern of cross ring and glycosidic bond cleavages that can be used to explain the masses of the fragment ions observed in the mass spectrum. These types of cleavages are similar to fragment patterns reported for other oligosaccharides.[43−48] We have recorded ion mobility distributions for individual fragments observed by selecting each with the quadrupole mass filter. Below, we use these results to assign the peaks observed in the ion mobility distributions recorded when the quadrupole is set to transmit all ions.[49]

Comparison of Ion Mobility Distributions Recorded with and without the Ion Trap. In order to assess the advantages of the ion trap interface, we have studied the efficiencies of recording ion mobility distributions with and without the trap. This comparison ultimately is limited by fluctuations in ion intensities. Typically, ion signals are relatively stable during a set of experiments and may vary by 10−20%; intensities without the trap depend heavily on focusing conditions, making day-to-day fluctuations in signal larger (as much as 50%). In order to prevent skewing of the data from mass discrimination that could arise at the ion trap, at the mass filter, or in the source, the quadrupole was fixed to transmit all ions for recording ion mobility distributions. We have repeated experiments with and without the trap several times. The improvents shown below are typical of those we observed and are much greater than any signal fluctuations.

Figure 3 shows a comparison of ion mobility distributions recorded for maltotetraose without the ion trap for 100 083 input pulses (20 μs in duration) and with the ion trap for 4003 input pulses (~1 μs in duration); both ion mobility distributions required the same data acquisition time (11 min), as discussed below. The results are quite striking. Both spectra show many resolved peaks that we have assigned by comparison with ion mobility distributions recorded for individual m/z ions.[50] Significantly more detail can be distinguished with the trap than without it. With the ion trap, we observe between 4 and 5 times larger signals while decreasing noise levels by similar factors. This is accomplished even though a factor of 25 fewer spectra were recorded (4003 with the trap, compared with 100 083 without), and the width of the ion pulse was reduced by a factor of ~20 (~1 μs with the trap, compared with 20 μs without).

(43) Spengler, B.; Dolce, J. W.; Cotter, R. J. *Anal. Chem.* **1990**, *62*, 1731.
(44) Ngoka, L. C.; Gal, J.-F.; Lebrilla, C. B. *Anal. Chem.* **1994**, *66*, 692.
(45) Yamagaki, T.; Ishizuka, Y.; Kawabata, S.; Nakanishi, H. *Rapid Commun. Mass Spetrom.* **1996**, *10*, 1887.
(46) Carroll, J. A.; Ngoka, L.; Beggs, C. G.; Lebrilla, C. B. *Anal. Chem.* **1993**, *65*, 1582.
(47) Lemoine, J.; Fournet, B.; Despeyroux, D.; Jennings, K. R.; Rosenberg, R.; de Hoffmann, E. *J. Am. Soc. Mass Spectrom.* **1993**, *4*, 197.
(48) Lipniunas, P. H.; Townsend, R. R.; Burlingame, A. L.; Hindsgaul, O. *J. Am. Soc. Mass Spectrom.* **1996**, *7*, 182.
(49) In the present experimental configuration, it is possible that some fragments are formed in the ion trap prior to ejection into the drift tube. This type of process should have a negligible effect on fragment ion drift times but could influence the relative abundances of different ions.
(50) A detailed study of ion mobility distributions recorded by mass-selecting individual m/z ions will be given elsewhere: Liu, Y.; Clemmer, D. E., manuscript in preparation. It is noteworthy that clear evidence of either multiple isomers or multiple conformations are observed for $m/z = 545$. This is similar to the behavior observed in the cyclodextrin systems (see ref 39).

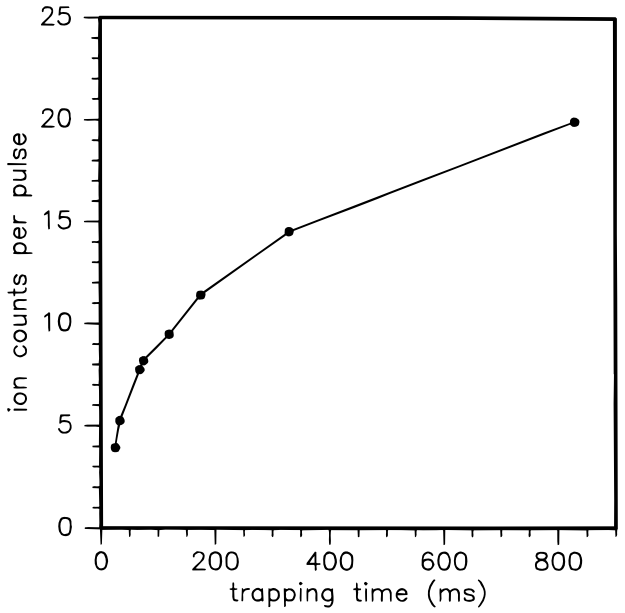

Figure 4. Ion counts per pulse plotted as a function of trapping time for ion mobility distributions recorded for maltotetraose under similar conditions used in Figure 3b. The ion signal per pulse was obtained by integrating the ion mobility distribution (recorded for all ions) and dividing by the number of ejected pulses.

One means of appraising the advantages of the ion trap method is to consider the duty cycles of the two experiments. Based on results for the ion trap TOFMS instruments, we expect that, for ejection pulses of ~1 μs, trapping times in excess of 10 ms should give duty cycles that approach 100%. For experiments with and without the ion trap, differences in focusing ions into the small aperture of the drift tube may influence the overall efficiencies of the experiments. For example, the nature of the tight spatial focusing that occurs in the ion trap may allow significantly more ions to be injected into the entrance aperture of the drift tube. A simple comparison of the pulse-out time as a function of the trapping time is not sufficient to characterize the true signals that are utilized in these experiments. Therefore, to deduce the true differences in signal intensities, we consider the total number of ions detected in experiments with and without the trap. Without the trap, the distribution recorded using a 20 μs pulse was repeated at 151.5 Hz, a duty cycle of only ~0.3%. As discussed in the introduction, this low duty cycle results because most of the ions are discarded during the ion mobility measurement. By integrating spectra with and without the ion trap and accounting for differences in the number of pulses recorded in each experiment, we conclude that, in Figure 3, we were able to trap and inject signals that were roughly 60% as intense as the total continuous ion signal that can be focused into the drift tube without the trap. Other with-trap and without-trap comparisons give values that range from 60 to 100%, similar to the expected duty cycles for these experiments.

A caveat concerning the above discussion is required because of the time necessary to trap ions. Without the trap, the repetition rate of experiments is defined by the mobilities of the ions being studied. The data that were recorded using 100 083 pulses (Figure 3) were acquired at a pulse frequency of 151.5 Hz; thus, the acquisition time was 11 min. With the ion trap, the experimental repetition rate is limited by the trapping time. The 4003 pulses recorded with the ion trap utilized a trapping time of 0.16 s; thus, these data also required an 11 min acquisition time.

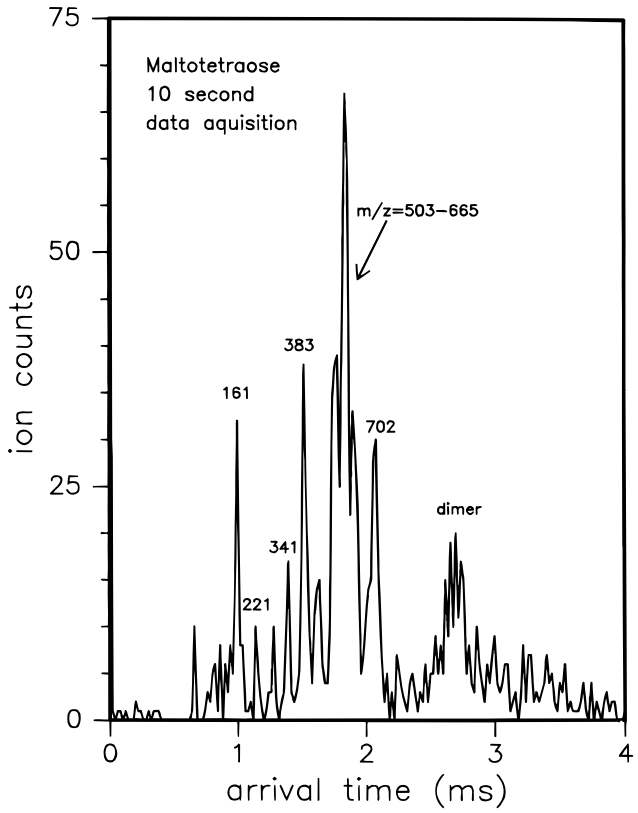

Figure 5. Ion mobility distribution recorded for maltotetraose ions recorded under similar trapping and injection conditions to those shown in Figure 3b. The dwell time resolution of the multichannel scaler was 20 μs/bin for these measurements. The data acquisition time was 10 s and corresponds to a sample consumption of ~80 pmol. Individual peaks are labeled with values of their mass-to-charge ratios determined in separate experiments, as mentioned in Figure 3.

Figure 4 shows a plot of the integrated ion counts per pulse (for all ions) that has been recorded as a function of trapping time. The ion signal per pulse increases with increasing trapping time, to the longest times we have studied, ~0.83 s. Ultimately, the best conditions for recording data depend on the type of experiment, since the data acquisition time is determined from both the trapping time and the experimental repetition rate.

Perhaps the simplest and most relevant assessment of the advantages of using an ion trap is to consider improvements in signal-to-noise (S/N) ratios for data recorded for the same length of time. This comparison shows that we have gained a factor of ~20 in S/N, an improvement that includes advantages that arise from trapping, and presumably, more efficient injection due to focusing that occurs in the trap. The S/N ratios of data recorded without the trap can be increased by a factor of 2 by using a 40 μs injection pulse. However, further increase in the pulse width decreases the resolution of the experiment. In all of our comparisons of data that were recorded for similar time periods with and without the trap, S/N improvements of factors of ~10–30 were obtained (with trapping).

Detection Limit and Possible Applications. With these improvements in signal, it is interesting to assess the detection limit of this method and useful applications. We find that a single ion pulse of maltotetraose can routinely be detected at a S/N level greater than 3:1 when trapping times of ~0.1 s are used. Taking into account solution concentrations and syringe pumping speeds, this corresponds to a sample consumption of only 1.3 pmol. These

detection limits suggest that ESI−ion mobility methods will be directly useful for detecting eluents from methods such as capillary electrophoresis or high-performance chromatographic methods, as has been proposed by Hill and co-workers.[6] One of the pitfalls of ion mobility spectrometry detection is that many ions have similar mobilities making it difficult to unambiguously identify samples solely on the basis of a single peak in the mobility distribution. The ability to collisionally induce fragmentation in the injected-ion approach offers advantages in identifying compounds. Figure 5 shows a rapidly acquired (10 s) ion mobility distribution in which at least 11 peaks, corresponding to singly charged ions of maltotetraose monomer, dimer, and fragments of the monomer, are clearly resolved. The purpose of this figure is to show the capability of this method for rapid sample characterization. The presence of mulitple peaks should make sample identification from ion mobility data alone substantially more definitive. This approach is similar to electron-impact ionization MS detection of separations carried out by gas and liquid chromatography, where fragment ions formed upon ionization are used to unambigously identify compounds. It should be kept in mind that, while this approach is conceptually similar to MS approaches, the ion mobility separation is based on collision cross section-to-charge ratios rather than m/z ratios. Thus, this method may have particular advantages in identifying different isomers, a problem that is particularly relevant in the analysis of oligosaccharides.[39]

CONCLUSIONS

We have shown that an ion trap interface for ESI−ion mobility experiments is a minor instrumental alteration that offers substantial advantages over the low-duty-cycle methods previously employed. In this report, we have made little attempt to optimize performance of the ion trap and have focused our discussion on improvements in recording ion mobility distributions for maltotetraose. In future studies, we will present a more thorough study of other experimental parameters that may influence instrumental performance, including (1) a thorough investigation of other ions; (2) variations in the buffer gas pressure and composition by adding gasses from an external source; (3) the influence of the trap's position with respect to the drift tube entrance aperture; and (4) comparison of signal intensities when ejection pulses are applied to the entrance or exit electrode of the trap. In the current configuration, we have obtained duty cycles of nearly 100%, which correspond to improvements in S/N of factors of 10−30 compared with data recorded without the trap. These improvements allow detection limits for maltotetraose of 1.3 pmol to be obtained. We have demonstrated the ability of ion mobility spectrometry to monitor collision-induced fragmentation of biomolecules. This method has similarities with MS methods of detection in that it is sensitive and can resolve an array of related fragment ions, allowing unambiguous sample characterization.

ACKNOWLEDGMENT

We are grateful to Dr. Yansheng Liu for many insightful discussions regarding the fragmentation of oligosaccharides. This work was supported by the National Science Foundation (Grant No. CHE-9625199).

Received for review May 21, 1997. Accepted July 31, 1997.[⊗]

AC970526A

[⊗] Abstract published in *Advance ACS Abstracts,* September 15, 1997.